Hindawi Publishing Corporation
Mathematical Problems in Engineering
Volume 2014, Article ID 916798, 16 pages
http://dx.doi.org/10.1155/2014/916798

Research Article

A New Model for Predicting Dynamic Surge Pressure in Gas and Drilling Mud Two-Phase Flow during Tripping Operations

Xiangwei Kong,[1] Yuanhua Lin,[2] Yijie Qiu,[1] Hongjun Zhu,[2] Long Dong,[3] and Yanchao Chen[4]

[1] *State Key Laboratory of Oil and Gas Reservoir Geology and Exploitation, Southwest Petroleum University, Chengdu, Sichuan 610500, China*
[2] *CNPC Key Lab for Tubular Goods Engineering, Southwest Petroleum University, Chengdu, Sichuan 610500, China*
[3] *Daqing Normal University and Petro China Daqing Oilfield Company, Daqing, Heilongjiang 163000, China*
[4] *No. 1 Oil Production Plant, Petro China Daqing Oilfield Company, Daqing, Heilongjiang 163000, China*

Correspondence should be addressed to Xiangwei Kong; m13880214723@163.com and Yuanhua Lin; yhlin28@163.com

Received 31 August 2013; Accepted 28 November 2013; Published 8 January 2014

Academic Editor: Lu Zhen

Investigation of surge pressure is of great significance to the circulation loss problem caused by unsteady operations in management pressure drilling (MPD) operations. With full consideration of the important factors such as wave velocity, gas influx rate, pressure, temperature, and well depth, a new surge pressure model has been proposed based on the mass conservation equations and the momentum conservation equations during MPD operations. The finite-difference method, the Newton-Raphson iterative method, and the fourth-order explicit Runge-Kutta method (R-K4) are adopted to solve the model. Calculation results indicate that the surge pressure has different values with respect to different drill pipe tripping speeds and well parameters. In general, the surge pressure tends to increase with the increases of drill pipe operating speed and with the decrease of gas influx rate and wellbore diameter. When the gas influx occurs, the surge pressure is weakened obviously. The surge pressure can cause a significant lag time if the gas influx occurs at bottomhole, and it is mainly affected by pressure wave velocity. The maximum surge pressure may occur before drill pipe reaches bottomhole, and the surge pressure is mainly affected by drill pipe operating speed and gas influx rate.

1. Introduction

Prospects of petroleum industry are the exploration and development of high pressure, formations pressures uncertainties, and abnormal permeability reservoirs [1, 2]. Managed pressure drilling (MPD) is often used in formations that have a narrow window between formation pore pressure and fracture pressure. Applying variations of MPD maintains the bottomhole pressure within the narrow window during the entire operation process, including drilling, and connections, tripping. To prevent formation influx or lost-circulation problems, wellbore pressures should be kept as constant as possible during the entire drilling process [3–5]. Tripping is a constant operation in the MPD, and moving drill pipe is accompanied by a displacement of the drilling mud in wellbore [6], so the movement of drill pipe in a wellbore filled with drilling mud can generate an additional pressure. The pressure produced by the downward movement of drill pipe is called surge pressure, while the pressure that decreased in the upward movement of drill pipe is called swab pressure. For the unstable moving velocity of the drill pipe, the generated surge pressure will affect the equilibrium relation of the pressure system in the wellbore. The bottomhole pressure fluctuates with the change of the surge pressure during the tripping operation. As the bottomhole pressure should be constant during the trip progress in MPD, it is necessary to accuratly calculate the surge pressure. The circulation loss or the other complex accidents can also be caused by the surge pressure for the high velocity of the drill pipe. The high drilling mud velocity and surge pressure may damage reservoir [7]. Many research data show that 25% of accidents

in the drilling operation are caused by surge pressure. It is suggested that excessive surge pressures have initiated lost circulation, formation fracturing, and well kick problems during the drilling operation. This may result in expensive drilling mud treating costs and cause other wellbore problems [8]. Obviously, the accurate calculation of surge pressure is related to the safety of the drilling process [9]. Also, there is a particular relationship between reasonable drilling mud density, well structural design, and surge pressure. Therefore, the surge pressure is very important basic parameters in drilling design [10]. So far, the calculation of surge pressure in drilling mud and gas is still worth continuing and in-depth research.

A number of field studies investigate the effects of wellbore geometry on surge pressures and drilling mud properties [11]. However, the first valid reports from surge pressure were not published until 1960, and the method to calculate the surge pressure began to apply to drilling industry [12]. A theoretical analysis of couette flow of power-law fluids for surge pressure was conducted by Chukwu in 1989 [13]. Model for both slot flow and concentric wellbore flow was developed for a stationary outer pipe and a steady axial motion of a concentric inner pipe. The inner pipe was assumed to be either plugged and of uniform geometry or open at the bottom. After the year, Fan [14] presented a method for accurate calculation of the surge pressure caused by drilling mud viscosity during tripping in a vertical wellbore in 1990. The models of laminar flow velocity profile and surge pressure of Newtonian and power law liquid in the wellbore are developed, and the drill pipe operating speed and drilling mud properties controlled for the safety of operation. In the same year, the method for calculating surge pressure under stable conditions was proposed by Zhou et al. [15], and the problem existing in the calculation curves for adhesive factor value was cited. In this research, the drilling mud is mainly composed of the power-law fluid and Bingham fluid. The calculation method for surge pressure under stable conditions is applicable by taking the compressibility of drilling mud and expansion of wellbore into consideration. In the article of Chukwu [16], a laminar couette flow model for power-law fluids through a slot was considered. Using the mathematical relationships developed, knowledge of the drilling mud rheological properties, drill pipe operating speed, and wellbore geometry is needed to determine the surge pressure. With consideration the compressibility of drilling fluids and wellbore, surge pressure was calculated by Jiang [17]. By using theoretical analysis and experimental results, it demonstrated that surge pressure is a function of well depth, the combination of drilling tools, wellbore diameter, properties of drilling mud, drill pipe operating speed and acceleration of drill pipe movement, and so forth. Next, a calculation method of surge pressure caused by drilling mud viscosity while the drill pipe moves through a Caisson drilling mud in wellbore was given by Wang et al. [18, 19]. The coefficients of surge pressure under different conditions are plotted. These results are useful in the control of drill pipe operating speed and the design of drilling mud properties. In the computational model, flow rate of drilling mud is considered as one-dimensional flow, and the method of characteristics and finite-difference technique are used to solve the basic equation of unsteady state flow. Meanwhile a theoretical model is presented by Fan et al. [20] for predicting dynamic surge pressure based on the theory of unsteady state flow in 1995. The basic partial differential equations for describing dynamic surge pressure are given. Fan methods are proposed for determining boundary and initial conditions when considering well parameters, drill bit, jet nozzles of drill bit, variability of tripping velocity, and acceleration. An example for the application of the model was also given [21, 22]. Bjørkevoll et al. [23] developed an easy to use transient surge swab model by taking into account dampening of pressure peaks due to fluid compression and elasticity of open wellbore. In this model, the contributions from acceleration are also included. When there is little gel strength in the fluid, the transient model reproduced relevant measured data with adequate accuracy. Recently, Nygaard et al. [24] present a new method for coordinated control of pump rates and choke valve for compensating surge pressure during tripping operations. Fedevjcyk et al. [25, 26] searched that wellbore diameter variations and the use of drill pipe accessories might cause changes to the annular cross-section space between the drill pipe and the borehole. This study proposes a mathematical/numerical model to simulate the surge pressure problem in wellbore with variable cross-section areas. The fluid flow yielded by the movement of drill pipe is considered to be one-dimensional, compressible, and transient. In order to predict the surge pressure caused in the horizontal well drilling process, Sun et al. [27] created models for predicting surge pressure based on the general theory of hydrostatic drilling mud mechanics and specifically described the flowing physical model towards surge pressure in horizontal wellbore by taking the effect of drill pipe eccentricity on the flowing law of drilling fluid into consideration. Lebele-Alawa and Oparadike [28] analyse the effects of surge pressure on pipe flow. The surge pressure investigated is that propagated by the emergency relief-coupling valve (ERV) connected to a loading system carrying crude oil from four flow stations. Kong et al. established the calculation model for fluctuation pressure in gas-liquid two-phase flow during tripping operations, but the model is just applicable to steady state conditions [29]. Crespo and Ahmed [30] reported recently the results of an experimental study aimed at investigating the effects of drill pipe speed, drilling mud properties, and wellbore geometry on surge pressures under laboratory conditions.

Although a large number of experiments under controlled laboratory conditions and modeling studies were conducted in the past to investigate surge pressures, the existing surge pressure models rarely take the impact of the gas into consideration and thus will inevitably affect the precision calculation for the surge pressure during MPD operations. If the gas influx occurs at the bottom of well, the surge pressure may be reduced greatly. The calculation method for predication of surge pressure in two-phase is not as accurate as the prediction of single-phase drilling mud due to its simplicity. In conclusion, we must take into account this problem rationally and place more emphasis on the surge pressure in two phases during MPD operations.

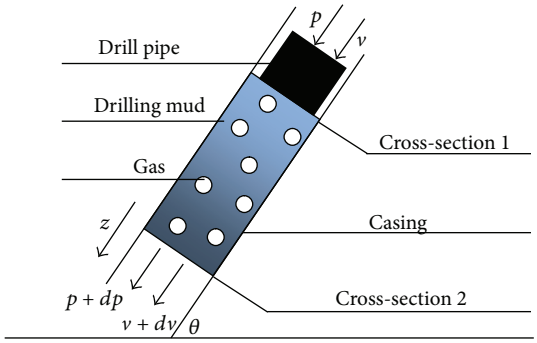

Figure 1: The schematic of gas and drilling mud two-phase flow during tripping operations.

The object of the present work is to present a new calculation model for predicting surge pressure during tripping operations, which is applicable for gas drilling mud two-phase fluid. In this paper, in addition to the pressure, temperature, and the void fraction in the wellbore, the compressibility of the gas phase, the wave velocity in real-time, the changes of wellbore parameter and three scenarios are also taken into consideration. By introducing the momentum conservation equations and the mass conservation equations in MPD operations, pressure wave velocity in real-time, gas-drilling mud equations of state (EOS), and a new model for predicting dynamic surge pressure in gas drilling mud two-phase during tripping operations is developed. Numerical solutions, difference method and characteristics method are obtained to solve the model. The model can be used to predict the change of the surge pressure at any well position at different influx rate, drill pipe operating speed, and drilling parameter.

2. The Mathematical Model

2.1. The Basic Equation. Drilling mud contains clay, cuttings, barite, other solids, and so forth. The solid particles are small and uniformly distributed; therefore, drilling mud is considered to be a pseudohomogeneous liquid, and the natural gas influx is considered to be the gas phase. As shown in Figure 1, the wellbore is filled with gas and drilling mud two-phase fluid. The downward movement of drill pipe along wellbore filled with drilling mud can create a surge of pressure. The two-phase drilling fluid and the passageway are all compressible and expansible. Therefore, the two-phase drilling fluid flow induced by the trip is unstable, especially in the deep well.

To establish the model about surge pressure during trip operations, the following assumptions are made:

(i) the two-phase flow is treated as one-dimensional;

(ii) no mass transfers between the gas and drilling mud;

(iii) the flow pattern in wellbore is either bubble or slug flow;

(iv) the annulus is concentric.

When drilling strings are moving in the wellbore full of drilling mud, the pressure gradient equations, the mass conservation equations and the momentum conservation equations along the flow direction in the wellbore is combined to study the surge pressure in tripping operations.

The mass conservation equation and momentum conservation equation are shown as follows:

$$pA + \rho_m g\left(A + \frac{\partial A}{\partial z}\cdot\frac{dz}{2}\right)dz\cdot\sin\theta + \left(p + \frac{\partial p}{\partial z}\cdot\frac{dz}{2}\right)\frac{\partial A}{\partial z} \cdot dz - \left(pA + \frac{\partial (pA)}{\partial z}dz\right) - \tau_0 X dz = \rho_m\left(A + \frac{\partial A}{\partial z}\cdot\frac{dz}{2}\right)dz\cdot\frac{dv}{dt}. \tag{1}$$

$$\frac{1}{\rho_m g}\frac{\partial p}{\partial z} + \frac{1}{g}\left(\frac{\partial v}{\partial t} + v\frac{\partial v}{\partial z}\right) + \frac{f v|v|}{8mg} = 0. \tag{2}$$

The total pressure drop gradient is the sum of pressure drop gradients due to potential energy change, kinetic energy, and frictional loss. From (2), the equation used to calculate pressure gradient of gas drilling mud two-phase flow within the wellbore can be written as

$$\frac{dp}{dz} = \rho_m g\sin\theta - \frac{\tau_w \pi D}{A} - \rho_m v_m \frac{dv_m}{dz}. \tag{3}$$

Assuming the compressibility of the gas is only related with the pressure in the wellbore, the kinetic energy and acceleration term in the equation above can be simplified to

$$\rho_m v_m \frac{dv_m}{dz} = -\frac{\rho_m v_m v_{sg}}{p}\frac{dp}{dz} = -\frac{W_m q_G}{A^2 p}\frac{dp}{dz}. \tag{4}$$

Substituting (3) into (4), the total pressure drop gradient along the flow direction within the wellbore can be expressed as

$$\frac{dp}{dz} = \frac{\rho_m g + \tau_f}{1 - W_m q_G/(A^2 p)}. \tag{5}$$

The continuity equations can be obtained directly based on (1):

$$c^2(P, T, D, \phi, w, Lg)\frac{\partial v}{\partial z} + \frac{1}{\rho_m}\frac{dp}{dt} + v\frac{\partial p}{\partial z} = 0, \tag{6}$$

where wave velocity $c(P, T, D, \phi, w, Lg)$ changes in real-time when the gas influx occurs at the bottom of drilling well.

The equations of motion can be obtained directly based on (2):

$$\frac{1}{\rho_m}\frac{\partial p}{\partial z} + \frac{\partial v}{\partial t} + g\frac{dv}{dz} + \frac{f v|v|}{2D} = 0. \tag{7}$$

2.2. Pressure Wave Velocity. Only consider the deformation of wellbore caused by surge pressure, the elastic constant of drill pipe is

$$\beta = \frac{2}{D_1\Delta p}\left(\frac{1-u_s}{E_s}\frac{\Delta p D_1^2}{D_2^2 - D_1^2}D_1 + \frac{1+u_s}{E_s}\frac{D_2^2 - D_1^2\Delta p}{D_2^2 - D_1^2}\frac{1}{D}\right). \tag{8}$$

The elastic constant of well wall is

$$\beta = \frac{2}{E_f}\left(1+\mu_f\right). \tag{9}$$

The elastic constant between well wall and drill pipe is

$$\beta = \frac{2}{R_2^2-1}\left[\frac{R_2^2}{E_f}\left(1+u_f\right)+\frac{1}{E_s}\left(\frac{R_1^2+1}{R_1^2-1}-u_s\right)\right]. \tag{10}$$

The elastic constant between casing and drill pipe is

$$\beta = \frac{2}{R_2^2-1}\left[\frac{R_2^2}{E_3}\left(\frac{R_3^2+1}{R_1^2-1}+u_3\right)+\frac{1}{E_2}\left(\frac{R_1^2+1}{R_1^2-1}-u_2\right)\right], \tag{11}$$

where $R_1 = D_2/D_1$, $R_2 = D_3/D_4$, and $R_3 = D_4/D_3$.

The density of gas and drilling mud mixture is described as the following formula:

$$\rho_m = \phi_G\rho_G + \phi_L\rho_L. \tag{12}$$

The small perturbation theory is also applied to the solution of wave velocity model. According to the solvable condition of the homogenous linear equations that the determinant of the equations is zero, the equation of pressure wave can be expressed in the following form [31]:

$$\begin{vmatrix} \left(\rho_g + c_p\phi_G\rho_L\frac{v_s^2}{c_g^2}\right)w & \frac{\phi_g}{c_g^2}\left[1-c_p\phi_L\right]\frac{v_s^2}{c_L^2}w & -\left[\phi_g\rho_g k + 2c_p\phi_g\phi_L\rho_L\frac{v_s}{c_L^2}w\right] & 22c_p\phi_g\phi_L\rho_L\frac{v_s}{c_L^2}w \\ -\rho_L w & \frac{1-\phi_G}{c_L^2}w & 0 & -k\left(1-\phi_G\right)\rho_L \\ \rho_L v_r^2 k\left(-\phi_G c_p + c_r - c_i + c_{m2}\right) & -\phi_G k\left[1-\phi_L\frac{c_p v_s^2}{c_L^2}+c_i\frac{v_s^2}{c_L^2}\right] & \phi_g\left(\rho_g + c_{vm}\rho_L\right)w & -c_{vm}\phi_g\rho_L w + i\left(\frac{3}{4}\frac{c_D}{r}\rho_L\phi_g v_s\right) \\ \rho_L v_s^2 k\left(\phi_L c_p - 2c_r - c_{m2}\right) & -k\left(\phi_L + c_r\phi_g\frac{v_s^2}{c_L^2}\right) & -c_{vm}\phi_g\rho_L w + i\left(\frac{3}{4}\frac{c_D}{r}\rho_L\phi_g v_s\right) & \rho_L\left[\phi_L+\phi_g c_{vm}\right]w \\ & & & -i\left(\frac{3}{4}\frac{c_D}{r}\rho_L\phi_g v_s + \frac{4}{D}f_{gw}\rho_g v_g\right) \\ & & & -i\left(\frac{3}{4}\frac{c_D}{r}\rho_L\phi_g v_s + \frac{4}{D}f_L\rho_L v_L\right) \end{vmatrix} = 0, \tag{13}$$

where $c_i = 0.3$, $c_p = 0.25$, $c_{m2} = 0.1$, and $c_r = 0.2$.

The real value of wave number is determined by the pressure wave velocity $c(P, T, D, \phi, w, Lg)$, and pressure wave velocity in the gas drilling mud two phase flow is

$$c\left(P,T,D,\phi,w,Lg\right) = \frac{\left|w/R^+(k) - w/R^-(k)\right|}{2}. \tag{14}$$

2.3. Physical Equations

2.3.1. Equations of State for Gas. The equation of state (EOS) for gas can be expressed as follows:

$$\rho_G = \frac{P}{\left(Z_G\cdot R\cdot T\right)}, \tag{15}$$

where Z_G is the compression factor of gas.

The formula presented by Dranchuk has been used to solve the compression factor under the condition of low and medium pressure ($P < 35$ MPa) [32]:

$$z_G = 1 + \left(0.3051 - \frac{1.0467}{T_r} - \frac{0.5783}{T_r^3}\right)\rho_r + \left(0.5353 - \frac{02.6123}{T_r} - \frac{0.6816}{T_r^3}\right)\rho_r^2, \tag{16}$$

where $T_r = T/T_c$, $p_r = p/p_c$, $\rho_r = 0.27p_r/Z_G T_r$.

The formula presented by Dranchuk and Abou-Kassem has been adopted to solve the compression factor under the condition of high pressure ($P \geq 35$ MPa) [32]:

$$z_G = \frac{0.06125P_rT_r^{-1}\exp\left(-1.2\left(1-T_r^{-1}\right)2\right)}{Y}, \tag{17}$$

where Y is given by

$$-0.06125P_rT_r^{-1}\exp\left(-1.2\left(1-T_r^{-1}\right)^2\right) + \frac{Y+Y^2+Y^3+Y^4}{(1-Y)^3} = \left(14.76T_r^{-1} - 9.76T_r^{-2} + 4.58T_r^{-3}\right)Y^2 - \left(90.7T_r^{-1} - 242.2T_r^{-2} + 42.4T_r^{-3}\right)Y^{(2.18+2.82T_r^{-1})}. \tag{18}$$

2.3.2. Equations of State for Drilling Mud. Under different temperature and pressure, the density of drilling mud can be obtained by the empirical formulas. If $T < 130^\circ$C, the density of drilling mud can be obtained by the following equation:

$$\rho_L = \rho_0\left(1 + 4\times10^{-10}P_L - 4\times10^{-5}T - 3\times10^{-6}T^2\right). \tag{19}$$

If $T \geq 130^{\circ}$C, the density of drilling mud is

$$\rho_L = \rho_0 \left(1 + 4 \times 10^{-10} P - 4 \times 10^{-5} T - 3 \times 10^{-6} T^2 + 0.4\left(\frac{T - 130}{T}\right)^2\right). \tag{20}$$

2.3.3. Correlation of Temperature Distribution. The temperature of the drilling mud at different depth of the wellbore can be determined by the relationship presented by Hasan and Kabir [33]:

$$T = T_{ei} + F\left[1 - e^{(z_{bh}-z)/A}\right] \times \left(-\frac{g \sin\theta}{g_c J c_{pm}} + N + g_T \sin\theta\right) + e^{(z_{bh}-z)/A}\left(T_{fbh} - T_{ebh}\right). \tag{21}$$

2.4. Flow Pattern Analysis. Based on the analysis of flow characteristics in the closed drilling system, it can be safely assumed that the flow pattern in wellbore is either bubble or slug flow. The pattern transition criteria for bubbly flow and slug flow given by Orkiszewski are used to judge the flow pattern in the gas-drilling mud two-phase flow [34].

For bubbly flow,

$$\frac{q_G}{q_m} < L_B. \tag{22}$$

For slug flow,

$$\frac{q_G}{q_m} > L_B, \qquad N_{GV} < L_s, \tag{23}$$

where q_m is the volumetric flow rate of two-phase flow and $q_m = q_G + q_L$.

The dimensionless numbers L_s and L_B are defined as

$$L_s = 50 + \frac{36 N_{GV} q_L}{q_G}, \qquad L_B = 1.071 - \frac{0.7277 v_m^2}{D}, \tag{24}$$

where

$$N_{GV} = v_s\left(\frac{\rho_L}{g\sigma_s}\right)^{0.25}. \tag{25}$$

Flow parameters such as void fraction, mixed density, and virtual mass force coefficient are discussed for specific flow pattern.

The correlation between void fraction and drilling mud holdup is expressed as

$$\phi_G + \phi_L = 1. \tag{26}$$

2.4.1. Bubble Flow. The average density of the mixture for bubble flow is

$$\rho_m = \phi_L \rho_L + \phi_G \rho_G. \tag{27}$$

The void fraction for bubble flow is determined by the following equation:

$$\phi_G = \frac{1}{2}\left[1 + \frac{q_m}{v_s A} - \sqrt{\left(1 + \frac{q_m}{v_s A}\right)^2 - \frac{4 q_G}{v_s A}}\right]. \tag{28}$$

The friction pressure gradient can be obtained from the following formula:

$$\tau_f = f\frac{\rho_L v_L^2}{2D}. \tag{29}$$

2.4.2. Slug Flow. The distribution coefficient of gas in the drilling mud phase is determined by

$$C_0 = \frac{0.00252 \lg\left(10^3 \mu_L\right)}{A^{1.38}} - 0.782 + 0.232 \lg v_m - 0.428 \lg A. \tag{30}$$

The average density of the mixture for slug flow is

$$\rho_m = \frac{W_m + \rho_L v_s A}{q_m + v_s A} + C_0 \rho_L. \tag{31}$$

The void fraction for slug flow is determined by the following equation:

$$\phi_G = \frac{q_G}{q_G + q_L}. \tag{32}$$

The friction pressure gradient can be obtained from the following formula:

$$\tau_f = f\frac{\rho_L v_m^2}{2D}\left(\frac{q_L + v_s A}{q_m + v_s A} + C_0\right). \tag{33}$$

2.5. Wellbore Characteristic Analysis. Effective diameter proposed by Sanchez [35] is

$$D = \frac{\pi\left(D_2^2 - D_1^2\right)/4}{\pi\left(D_2 + D_1\right)/4} = D_2 - D_1. \tag{34}$$

The effective roughness of the wellbore can be expressed as

$$k_e = k_0 \frac{D_2}{D_2 + D_1} + k_i \frac{D_1}{D_2 + D_1}. \tag{35}$$

With D_i and D_o being the diameters of inner pipe and outer pipe, respectively, the k_0 and k_i are the roughness of outer pipe and the inner pipe, respectively.

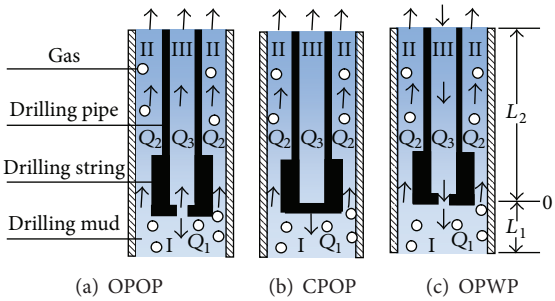

Figure 2: Different pipe end conditions in trip operations.

3. Boundary Conditions and Initial Conditions of the Model

When the drill pipe runs into the wellbore filled with drilling mud and gas at high velocities, there are three scenarios for the movement of the drill pipe. They are closed pipe without pumping (CPOP), open pipe without pumping (OPOP), and open pipe with pumping (OPWP), respectively. The three scenarios are illustrated in Figure 2. As drill pipe is moved downward into a wellbore, the drilling mud will move upward. To analyze the transient flow in the wellbore caused by the downward movement of drill pipe according to (6) and (7) and calculate the surge pressure at that time, it is indispensable to obtain the definite conditions of the model for the three scenarios, that is, initial conditions and boundary conditions.

We established coordinate systems of the hydraulic system in the wellbore. The coordinate systems have their origin at the end of the drill pipe. The flow rate of gas and drilling mud two-phase in open borehole, annulus (comprised by drill pipe and the casing), and drill pipe were, respectively, defined as Q_1, Q_2, and Q_3. Respectively, the corresponding passageways filled with gas and drilling mud two-phase fluid were marked as *I, III, and II,* andthe pressure is P_1, P_2, and P_3. The positive direction of passageway I was towards the bottomhole, while the positive directions of the passageway *III* and *II* were towards the wellhead. As seen in Figure 2, L_1 was the length from the origin to the bottomhole, and L_2 was the length from the origin to the wellhead. By calculating the velocity of two phases flow, the new model for surge pressure in gas-drilling mud two-phase during the movement of drill pipe can be deduced [36].

In actual hydraulic system of the well, many pipeline series are included. By assuming the length between the nodes and origin as L_3, the boundary consistency conditions are provided by

$$\begin{aligned} Q_i^{J+1}(L_3) - Q_i^J(L_3) &= v_p \cdot \Delta A \\ p_i^{J+1}(L_3) &= p_i^J(L_3) \end{aligned} \quad (i = 1, 2, 3). \tag{36}$$

According to the relationship between the pressure and velocity at the wellbore, the boundary conditions can be determined as follows:

$$\begin{aligned} p_i(L_2) &= 0 \\ Q_i(L_1) &= 0 \end{aligned} \quad (i = 2, 3). \tag{37}$$

The effective cross-area of jet nozzles is

$$A_e = \frac{1}{4}\pi \sum_{i=1}^{n} d_i^2. \tag{38}$$

3.1. OPOP Scenario. The following equation presents the initial conditions of the flow rate and pressure for OPOP scenario:

$$\begin{aligned} p_i(z) &= 0 \\ Q_i(z) &= 0 \end{aligned} \quad (i = 1, 2, 3). \tag{39}$$

The boundary conditions of the flow rate and pressure are

$$\begin{aligned} &Q_1(0,t) + Q_2(0,t) + Q_3(0,t) = v_p(t)(A_0 - A_3), \\ &p_1(0,t) = p_2(0,t), \\ &p_1(0,t) - p_3(0,t) \\ &= \frac{\rho_m}{2\mu_m}\left(\frac{Q_3(0,t)}{A_e} + v_p(t)\right)\left|\frac{Q_3(0,t)}{A_e} + v_p(t)\right|. \end{aligned} \tag{40}$$

3.2. CPOP Scenario. The following equation presents the initial conditions of the flow rate and pressure for CPOP scenario.

The initial conditions of the flow rate and pressure are as follows:

$$\begin{aligned} &p_1(z,0) = 0, \qquad Q_1(z,0) = 0 \\ &p_2(z,0) = \frac{f_2 z \rho_m Q_w^2}{8 m_2 A_2}, \qquad Q_2(z,0) = Q_w \\ &p_3(z,0) = \frac{f_3(L_2 - z)\rho_m Q_w^2}{8 m_3 A_3}, \qquad Q_3(z,0) = Q_w. \end{aligned} \tag{41}$$

The boundary conditions of the flow rate and pressure can be written in the following form:

$$\begin{aligned} Q_1(0,t) + Q_2(0,t) &= v_p(t) A_0 \\ Q_3(0,t) &= -v_p(t) A_3 \\ p_1(0,t) &= p_2(0,t). \end{aligned} \tag{42}$$

3.3. OPWP Scenario. As shown in Figure 2(c), the OPWP scenario is discussed below.

Excluding atmospheric pressure, the initial conditions at the wellhead and bottom hole are

$$\begin{aligned} &p_1(z,0) = 0, \qquad Q_1(z,0) = 0 \\ &p_2(z,0) = \frac{f_2 z \rho_m Q_w^2}{8 m_2 A_2}, \qquad Q_2(z,0) = Q_w \\ &p_3(z,0) = \frac{f_3(L_2 - z)\rho_m Q_w^2}{8 m_3 A_3}, \qquad Q_3(z,0) = Q_w. \end{aligned} \tag{43}$$

The boundary conditions of the flow rate and pressure are as follows:

$$Q_1(0,t) + Q_2(0,t) = v_p(t)(A_0 - A_3) + Q_w(0,t)$$
$$Q_3(0,t) = -v_p(t)A_3 + Q_w(0,t) \quad (44)$$
$$p_1(0,t) = p_2(0,t).$$

4. Solution of the United Model

Referring to Figure 4, the variable x is defined as a short pipe, and the constraint is $L_x < c_x \cdot \Delta t$. The variables y and z are short pipe which are made up of wellbore and drill pipe, and the constraint is $L_y < c_y \cdot \Delta t$, $L_z < c_z \cdot \Delta t$. The variables $x+1$, $y+1$ and $z+1$ are defined as a long pipe, and the constraint is $L_x + 1 < c_x + 1 \cdot \Delta t$, $L_y + 1 < c_y + 1 \cdot \Delta t$, $L_z + 1 < c_z + 1 \cdot \Delta t$. The implicit finite-difference method is applied to calculate the short pipe, and characteristics method is applied to calculate the long pipe. The pressure and flow rate can be obtained at the end of drill pipe as follows:

$$[p_{2,t}]_2 - \rho_m \left[\frac{c_{y+1}}{A_{y+1}} Q_{2,t}^{y+1}\right]_2 - \left\{[p_{3,t-\Delta t}]_2 - \rho_m \left[\frac{c_{y+1}}{A_{y+1}} Q_{t-\Delta t}\right]_2 + \frac{\rho_m \Delta t}{8}\left[\frac{c_{y+1}}{m_{y+1}} f_{3,t-\Delta t} v_{3,t-\Delta t} |v_{3,t-\Delta t}|\right]_2\right\} = 0,$$

$$[p_{2,t}]_3 - \rho_m \left[\frac{c_{z+1}}{A_{z+1}} Q_{2,t}^{z+1}\right]_3 - \left\{[p_{3,t-\Delta t}]_3 - \rho_m \left[\frac{c_{z+1}}{A_{z+1}} Q_{3,t-\Delta t}\right]_3 + \frac{\rho_m \Delta t}{8}\left[\frac{c_{z+1}}{m_{z+1}} f_{3,t-\Delta t} v_{3,t-\Delta t} |v_{3,t-\Delta t}|\right]_3\right\} = 0,$$

$$[p_{2,t}]_1 - \rho_m \left[\frac{c_{x+1}}{A_{x+1}} Q_{2,t}^{x+1}\right]_1 - \left\{[p_{3,t-\Delta t}]_1 - \rho_m \left[\frac{c_{x+1}}{A_{x+1}} Q_{3,t-\Delta t}\right]_1 + \frac{\rho_m \Delta t}{8}\left[\frac{c_{x+1}}{m_{x+1}} f_{3,t-\Delta t} v_{3,t-\Delta t} |v_{3,t-\Delta t}|\right]_1\right\} = 0,$$

$$[p_{2,t} + p_{1,t}]_2 + D_{11}\left[Q_{2,t}^y + Q_{1,t}^y\right]_2 + D_{12} = 0,$$
$$[p_{2,t} - p_{1,t}]_2 + E_{11}\left[Q_{2,t}^y - Q_{1,t}^y\right]_2 + E_{12} = 0,$$
$$[p_{2,t} + p_{1,t}]_3 + D_{21}\left[Q_{2,t} + Q_{1,t}^z\right]_2 + D_{22} = 0,$$
$$[p_{2,t} - p_{1,t}]_3 + E_{21}\left[Q_{2,t} - Q_{1,t}^z\right]_2 + E_{22} = 0,$$
$$[p_{2,t} + p_{1,t}]_1 + D_{31}\left[Q_{2,t} - Q_{1,t}^x\right]_1 + D_{32} = 0,$$
$$[p_{2,t} - p_{1,t}]_1 + E_{31}\left[Q_{2,t} + Q_{1,t}^x\right]_1 + E_{32} = 0,$$

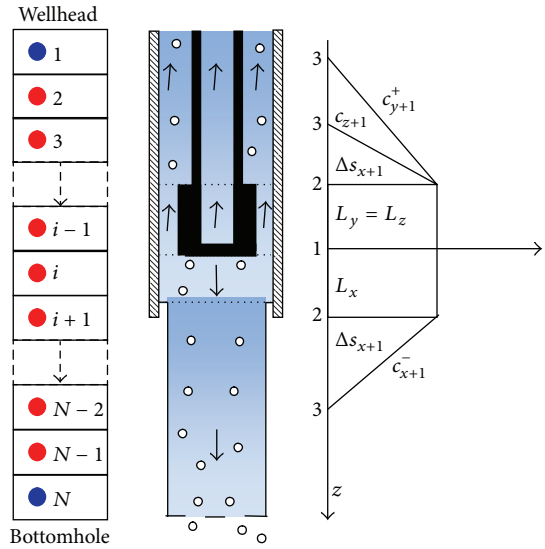

Figure 3: Schematic diagram of the solve.

$$[Q_{1,t}]_1 + [Q_{1,t}]_2 + [Q_{1,t}]_2 - v_{p(t)} \cdot (A_0 - A_i) = 0,$$
$$[p_{1,t}]_1 - [p_{1,t}]_3 - \frac{\rho_m}{2(uA_e)^2} \times \left\{[Q_{1,t}]_3 + A_e v_{p(t)}\right\}\left|[Q_{1,t}]_3 + A_e v_{p(t)}\right| = 0,$$
$$Q_{2,t}^{y+1} - Q_{2,t}^y - v_{p(t)} \cdot \Delta A = 0,$$
$$[p_{1,t}]_1 = [p_{1,t}]_2,$$
$$D_{11} = \frac{\rho_m c^2}{A} \cdot \frac{\Delta t}{L_J},$$
$$D_{12} = \frac{\rho_m}{A} \cdot \frac{L_J}{L_J}. \quad (45)$$

The D_{kj}, E_{kj} can be expressed as follows:

$$D_{i,t} = -(p_{i+1,t-\Delta t} + p_{i,t}) + D_{11}(Q_{i+1,t-\Delta t} - Q_{i,t-\Delta t}),$$
$$E_{i,t} = -(p_{i+1,t-\Delta t} + p_{i,t}) + E_{11}(Q_{i+1,t-\Delta t} - Q_{i,t-\Delta t}) + \frac{\rho_m f L_J}{16m}(v_{i+1,t-\Delta t} + v_{i,t-\Delta t})|(v_{i+1,t-\Delta t} + v_{i,t-\Delta t})|, \quad (46)$$

where $k = 1, 2, 3$ and $j = 1, 2$.

Obtaining the analytical solution of the mathematical models concerned with flow pattern, void fraction, parameters, and pressure drop gradient are generally impossible for most practical in two-phase flow. In this paper, the Runge-Kutta method (R-K4) is used to discrete the new model for surge pressure. At different wellbore depths, we can obtain pressure, temperature, gas velocity, drilling mud velocity, and

void fraction in MPD operations by application of the R-K4. The solution of pressure drop gradient equation (3) can be seen as an initial-value problem of the ordinary differential equation

$$\frac{dp}{dz} = F(z, p)$$
$$p(z_0) = P_0. \tag{47}$$

With the initial value (z_0, p_0) and the function $F(z, p)$, (3)–(5) can be obtained:

$$k_1 = F(z_0, p_0),$$
$$k_2 = F\left(z_0 + \frac{h}{2}, p_0 + \frac{h}{2}k_1\right),$$
$$k_3 = F\left(z_0 + \frac{h}{2}, p_0 + \frac{h}{2}k_2\right), \tag{48}$$
$$k_4 = F(z_0 + h, p_0 + hk_3),$$

where h is the step of depth. The pressure on the nod $i = i + 1$ can be obtained by

$$p_1 = p_0 + \Delta p = p_0 + \frac{h}{6}(k_1 + 2k_2 + 2k_3 + k_4). \tag{49}$$

In the present work, the surge pressure calculation model solved by personally compiled code on VB.NET (Version 2010). The schematic diagram of solve is shown in Figure 3, and the solution procedure for the surge pressure in the wellbore is shown in Figure 4. At initial time, the wellhead temperature, wellbore structure, well depths, gas and drilling mud two-phase properties, and so forth are known. On the node i, the pressure gradient, wave velocity varieties in real-time, temperature, and the void fraction can be obtained by adopting R-K4. The density of gas can be obtained by gas EOS (15), and the density of drilling mud can be obtained by equations (19) and equations (20). Then, the surge pressure at different depths of wellbore in tripping operations can be solved by (45). The process is repeated until the surge pressure in the whole wellbore has been obtained [37, 38].

The developed model takes full consideration of the gas influx and wave velocity in real-time. Owing to the complex conditions of wellbore in tripping operations, measurement of surge pressure in the actual drilling process is very difficult. In order to verify the new model for surge pressure, the predicted surge pressure is compared with the results of previous experimental investigations presented by Junfang in tripping operations in Figure 5 [39]. The comparisons reveal that the developed new model fits well with the experiments data. Thus, the new model can be used to accurately predict surge pressure on different scenario and gas influx rate in tripping operations. The value of surge pressure calculated by adopted Burkhardt's steady method is larger than the experiments data.

Table 1: Parameters of calculation well.

Type	Property	Value
Mud	Dynamic viscosity (Pa·s)	0.056
	Density (kg/m^3)	1460
Gas	Relative density	0.65
	Viscosity (Pa·s)	1.14×10^{-5}
String	Elastic modulus of string (Pa)	2.07×10^{11}
	Poisson ratio of string	0.3
	Roughness (m)	1.54×10^{-7}
Surface condition	Surface temperature (K)	298
	Atmosphere pressure (MPa)	0.101

5. Analysis and Discussion

The drilling system described is a closed system. The schematic diagram of gas influx process in tripping operations is illustrated in Figure 6. The drilling mud is pumped from surface storage, down the drill pipe, returns from the annulus, and travels back through surface processing, where drilling solids are removed, to surface storage.

The well used for calculation is a gas well in Xinjiang Uygur Autonomous Region, China. The wellbore structure, well design parameters (depths and diameters), gas and drilling mud two-phase properties (density and viscosity), and operational conditions of calculation well are displayed in Table 1 [40].

The drilling mud mixed with gas is considered as a two-phase flow medium. The surge pressure in the gas-drilling mud are calculated and discussed by using the established model and well parameters. As shown in Figure 7, according to the drill conditions, such as the drill pipe velocity, gas drilling mud two-phase flow velocity, the total length of drill pipe, and drill pipe is 1000 m, we can account for the changing rules of surge pressure. The following examples illustrate that the surge pressure is affected by different well parameters, drilling mud density, gas influx rate, and well depth in the tripping operations.

5.1. The Effects of Various Drilling Parameters on Surge Pressure. Figure 7 presents the influence of acceleration on drilling mud velocity, drilling mud velocity, and drill pipe operating speed with respect to the drilling parameters. The movement of drill pipe starts at the depth of 1000 m. With the movement of the drill pipe, the drilling mud also moves in the opposite direction along wellbore at the same time. The drill pipe operating speed reaches the maximum value at 23 seconds and stops at 30 seconds. In order to make a comparison of the surge pressure in different well parameters, the analysis and compared Figures 8–15 based on the data of Figure 7.

Figures 8 and 9 graphically show the distributions of void fraction and variations of wave velocity along the flow direction in the wellbore. When gas influx occurs at the bottom of well, some gas invades into the wellbore and migrates form the bottomhole to the wellhead along the flow direction. At low gas influx rate, it is extremely obvious that

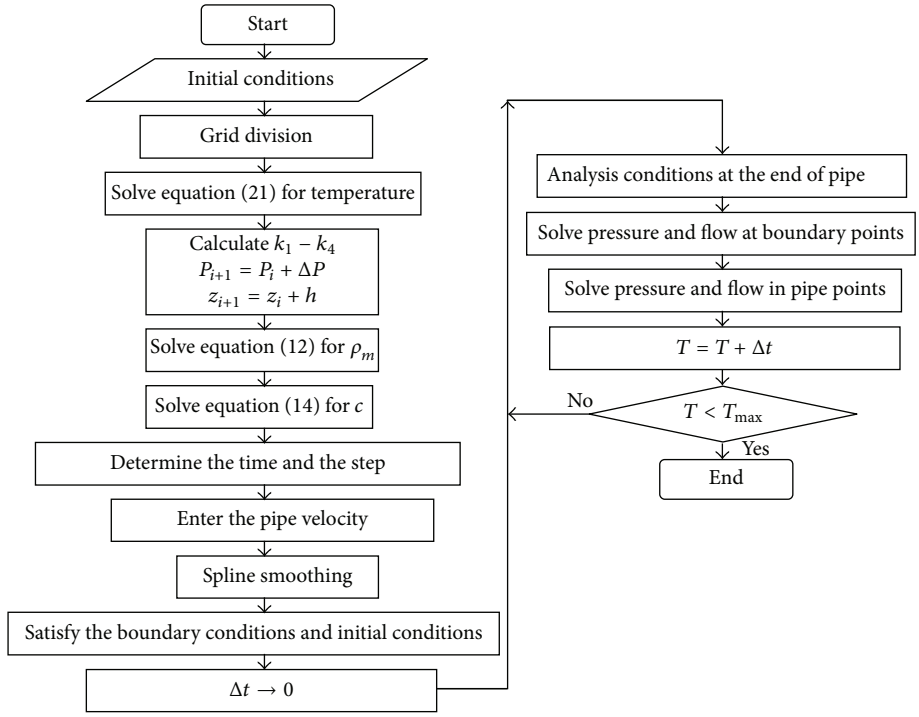

Figure 4: Solution procedure for surge pressure in MPD operations.

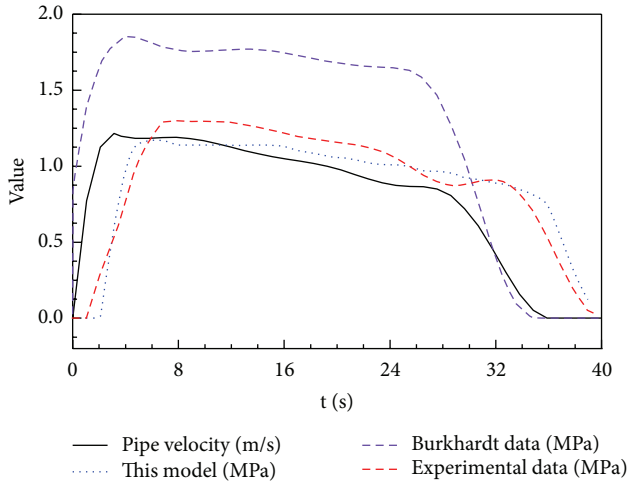

Figure 5: Experimental verification by comparison with previous experiment data.

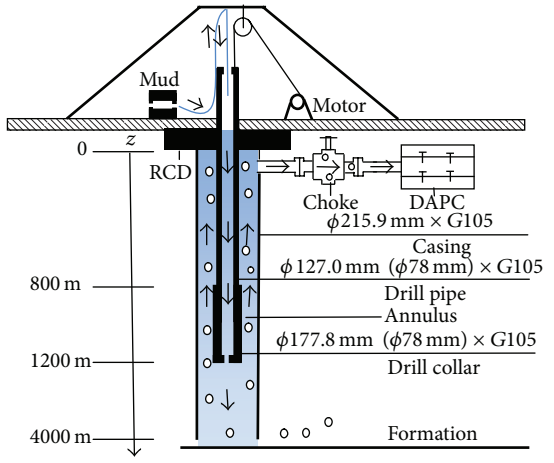

Figure 6: Schematic diagram of gas influx process in tripping.

the void fraction and wave velocity first slightly change in a comparatively smooth value then change sharply. It is because the volume of gas expanded rapidly with the decreasing of pressure near the wellhead, the void fraction increases sharply, and at the same time the wave velocity decreases obviously. At a high gas influx rate, the wave velocity tends to increase because the void fraction in the wellhead is increased to a high extent. In conclusion, the wave velocity is sensitive to the void fraction, and the void fraction is dominated by influx rate and pressure in the wellbore, especially the influx rate.

As shown in Figure 9 within the range of low gas influx rate, the wave velocity decreases significantly. It is because the compressibility of the gas increases remarkably, and the medium appears high elasticity, though the density of gas-drilling mud two-phase flow changes slightly. With the increase of gas influx rate and corresponding increase of the void fraction in the wellbore, the compressibility of the two-phase unceasingly increases, which promotes the momentum and energy exchange in the interface. Therefore, the wave velocity continuously decreases.

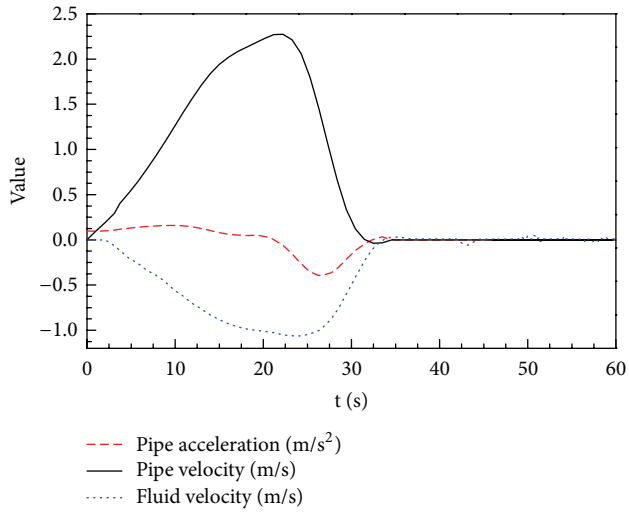

Figure 7: Drill pipe velocity variation at different accelerations.

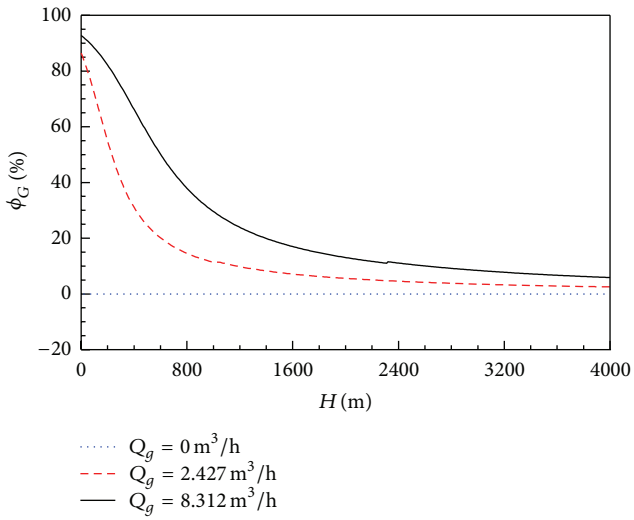

Figure 8: Void fraction distribution at different gas influx rates.

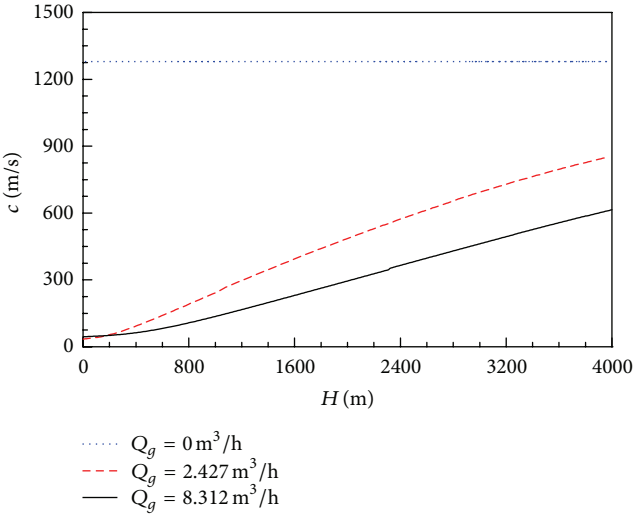

Figure 9: Wave velocity variation at different gas influxes.

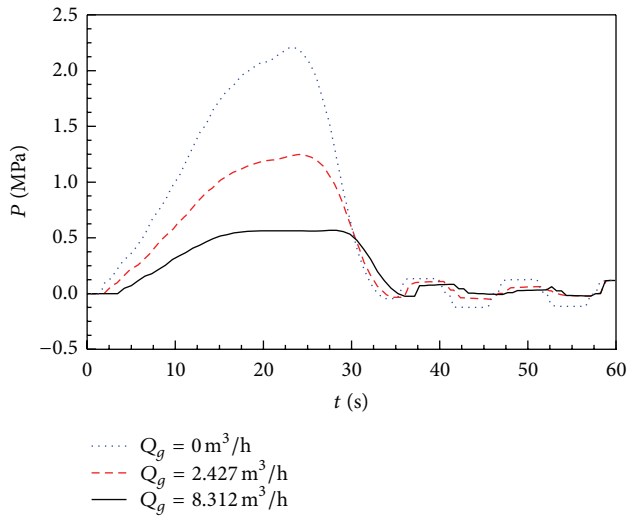

Figure 10: Surge pressure variation at different gas influxes.

Figure 10 illustrates the effect of gas influx on the surge pressure with the change of gas influx rate. As shown in Figure 10, under different gas influx rates (0 m^3/h, 2.427 m^3/h and 8.312 m^3/h, resp.) the maximum surge pressure may occur before drill pipe reaches bottomhole. With the increases of the gas influx, the corresponding surge pressure decreases. Considering the gas influx in the calculation of the surge pressure in the wellbore, the surge pressure weakens obviously. As the gas influx rate decreases, the surge pressure at bottom of the wellbore is reduced gradually, while surge pressure can cause a significant time lag if the gas influx occurs at the bottom of well. The lag time is mainly affected by wave velocity.

Figure 11 presents a change of surge pressure in the wellbore at different scenario (OPOP, CPOP, and OPWP, resp.). According to Figure 11, surge pressure is increased in CPOP scenario by comparing with the surge pressure in OPOP scenarios. It is because the speed of the drilling mud increases remarkably in CPOP scenario, the surge pressure becomes larger obviously. Especially when the maximum surge pressure occurs, a strong increase of surge pressure is observed at OPWP scenario. If the movement of drill pipe is stop immediately, the surge pressure will not disappear immediately, and the surge pressure will exist and change slightly for short while.

Figures 12 and 13 show that the surge pressure varies with wellbore diameter, caused by the drill pipe operating speed according to Figure 7. The surge pressure decreases with the increase of wellbore diameter. It is because the drilling mud flow rate decreases with the increases of wellbore diameter. Based on (1) and (2), surge pressure decreases at each position due to the decrease of drilling mud flow rate. Surge pressure caused by converting of potential energy into kinetic energy, and then kinetic energy back into potential energy, over and over again. During the tripping operations, especially in slim wellbore drilling process, the speed of drill pipe movement should be appropriately reduced. The surge pressure in

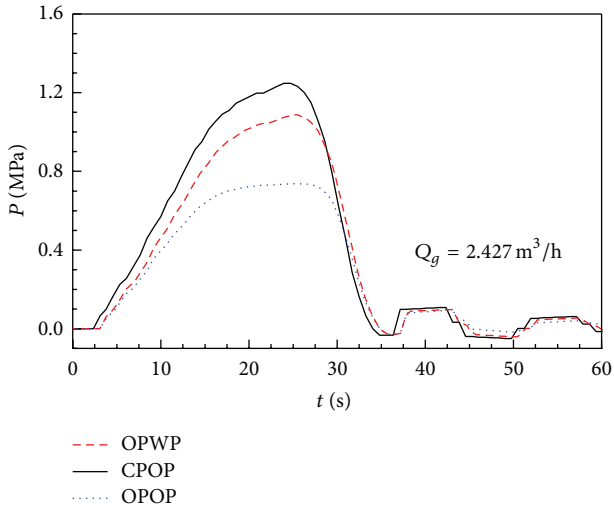

Figure 11: Surge pressure variation at different scenarios.

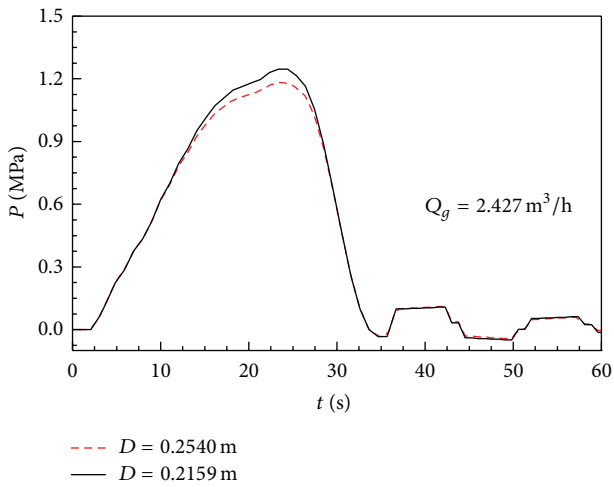

Figure 12: Surge pressure variation at different wellbore diameters (gas influx Q_g = 2.427 m^3/h).

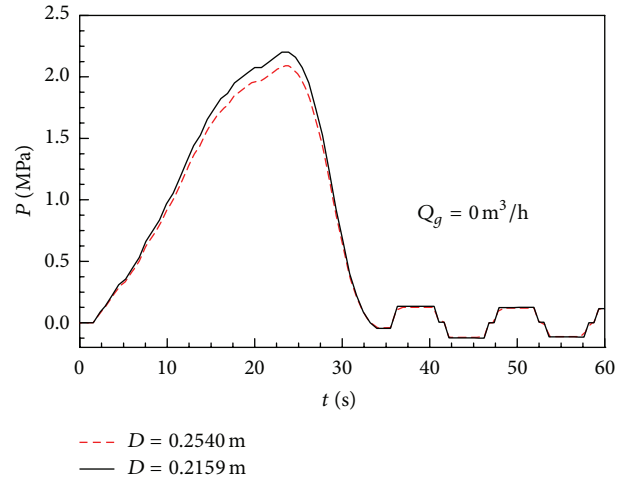

Figure 13: Surge pressure at different borehole diameters (gas influx Q_g = 0 m^3/h).

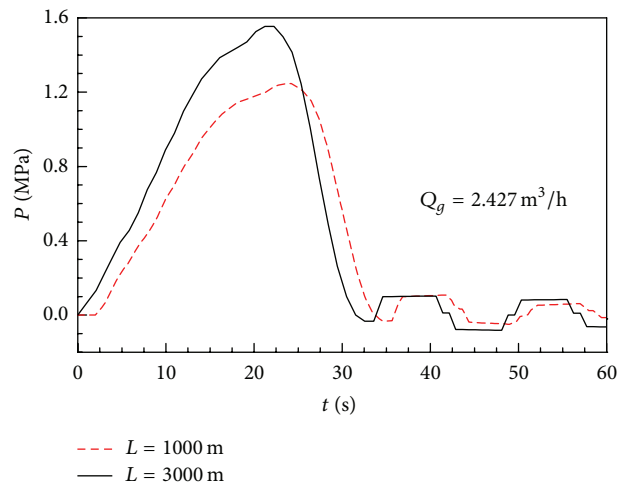

Figure 14: Surge pressure variation at different well depths.

Figure 13 is prominently larger than that in Figure 12. This is because both the decrease of the wave velocity and the increase of the compression in gas drilling mud two-phase due to the gas influx result in the comparatively large surge pressure.

Figure 14 illustrates that the surge pressure varied with the length of drill pipe. The surge pressure caused by shorter drill pipe (whose the total length is 1000 m) is smaller than the longer drill pipe (whose total length is 3000 m) before the maximum surge pressure occurs. This can explain that surge pressure is affected by the friction force of drill pipe and wellbore. Compared with the longer drill pipe, the friction force caused by shorter drill pipe is larger. Therefore, the surge pressure gradually decreases. As a result, the surge pressure is greater at 1000 m.

Figure 15 illustrates that the surge pressure varied with the drilling fluid density. At the bottom of well, the surge pressure increases with the increase of drilling fluid density. The changes are significant in the maximum surge pressure. This is because the surge pressure is mainly affected by wave velocity, density, and velocity of gas drilling mud two-phase. According to (6) and (7), the surge pressure is increased as the drilling fluid density increases. The maximum surge pressure occurs before drill pipe reaches bottomhole.

5.2. The Effects of Gas Influx Rate on Surge Pressure. Figures 16, 17, and 18 illustrate that the surge pressure varied with the increase of the gas influx rate. Figure 17 shows the surge pressure with the gas influx rate of 2.427 m^3/h at the bottom of well. Figure 18 shows the surge pressure with the gas influx rate of 8.312 m^3/h at the bottom of well. Mainly affected by wave velocity, density, and velocity in gas-drilling mud two phase, the surge pressure is greatest at the gas influx rate of 0 m^3/h. Figure 16 illustrates an example of a minimum wave velocity at the gas influx rate of 8.312 m^3/h at the bottom

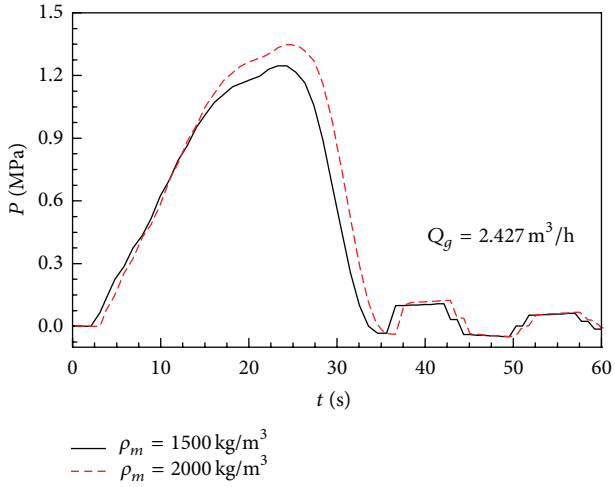

Figure 15: Surge pressure variation at different drilling fluid densities.

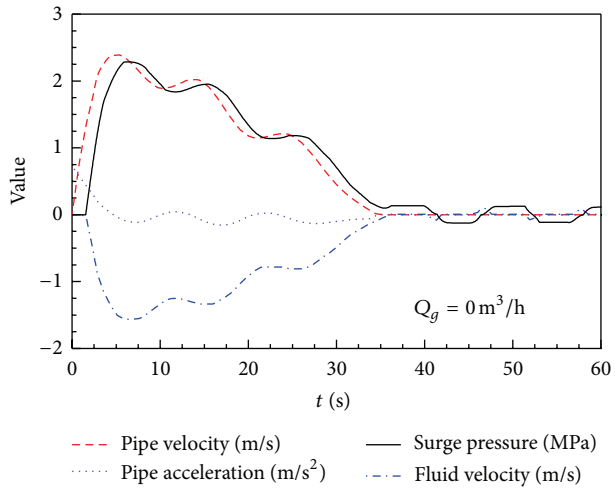

Figure 16: Surge pressure variation at different pipe velocities (gas influx Q_g = 0 m^3/h).

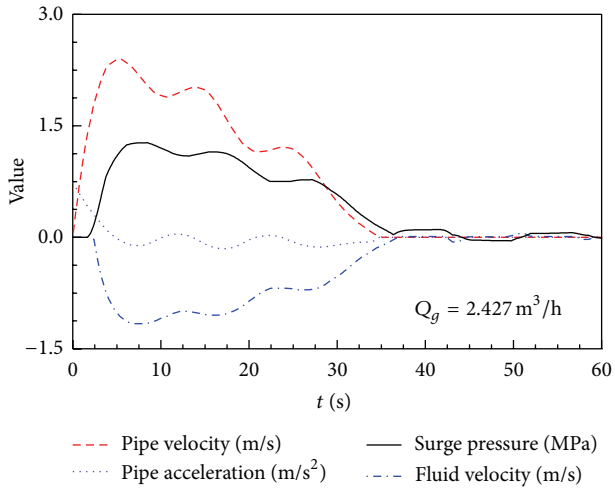

Figure 17: Surge pressure variation at different pipe velocities (gas influx Q_g = 2.427 m^3/h).

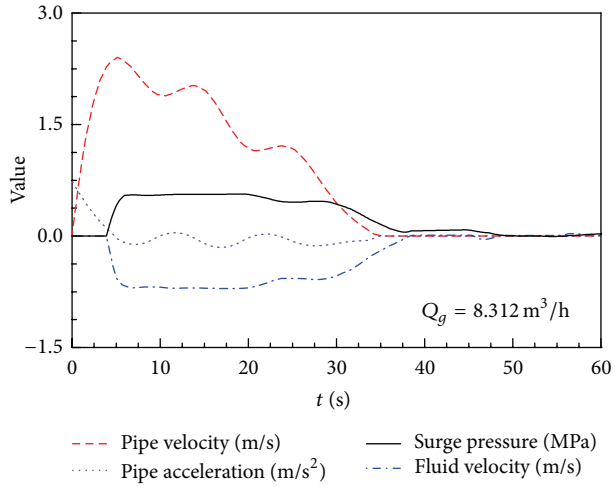

Figure 18: Surge pressure variation at different pipe velocities (gas influx Q_g = 8.312 m^3/h).

of well. As the gas influx rate increases, the surge pressure decreases. When gas influx occurs, the lag time is lengthened remarkably compared with the condition of no gas influx. The longer the distance is, the greater the lag time will be. The lag time is mainly determined by the propagation time of pressure wave in the wellbore.

Figures 19 and 20 illustrate the surge pressure caused by different operating speeds of the drill pipe at various gas influx rates at the bottom of well. As drilling mud mixed with influx gas not only reduces the pressure wave velocity but also reduces the density of the mixture density, surge pressure mainly affected by wave velocity and mixture density reduces drastically with the increase of gas influx rate at the bottom of well. Figures 19 and 20 are compared to Figures 17 and 18; it can be concluded that the operating speed is also a major factor of surge pressure.

5.3. The Effects of Drill Pipe Operating Speed on Surge Pressure. Figure 21 illustrates the effect of drill pipe speed on the surge pressure. The change of surge pressure is smaller in gas drilling two-phase than in single-phase drilling mud. The surge pressure becomes smaller and closes to zero after the movement is stopped due to greater friction force existing in well wall during drill pipe operating.

6. Conclusions

With full consideration of the important factors such as wave velocity in real-time, the compressibility of the gas phase, gas influx rate, pressure, temperature, and well parameters, a new surge pressure model has been proposed based on the

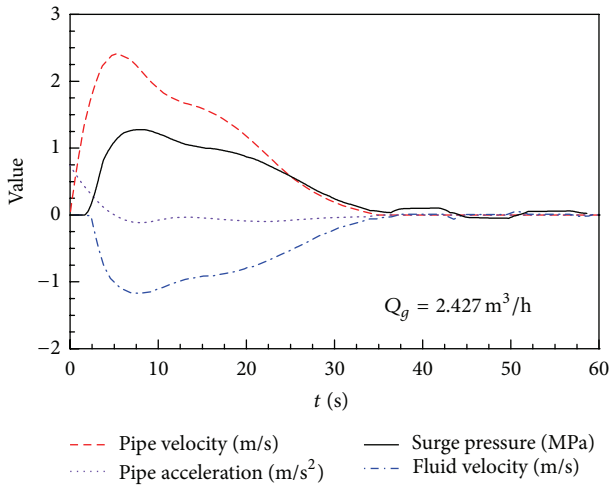

Figure 19: Surge pressure and fluid velocity variation at different pipe velocities (gas influx Q_g = 2.427 m^3/h).

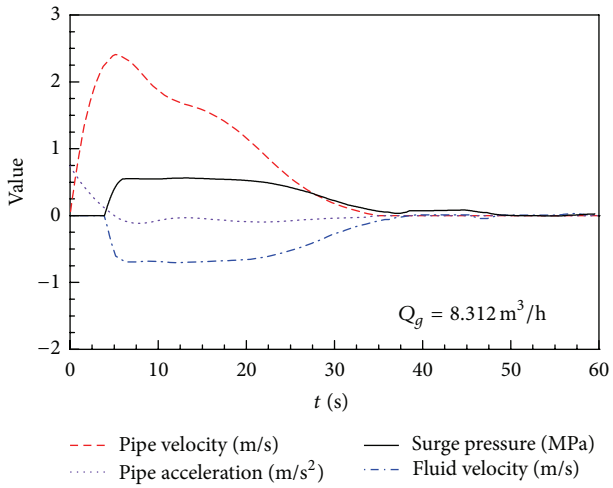

Figure 20: Surge pressure and fluid velocity variation at different gas influxes (gas influx Q_g = 8.312 m^3/h).

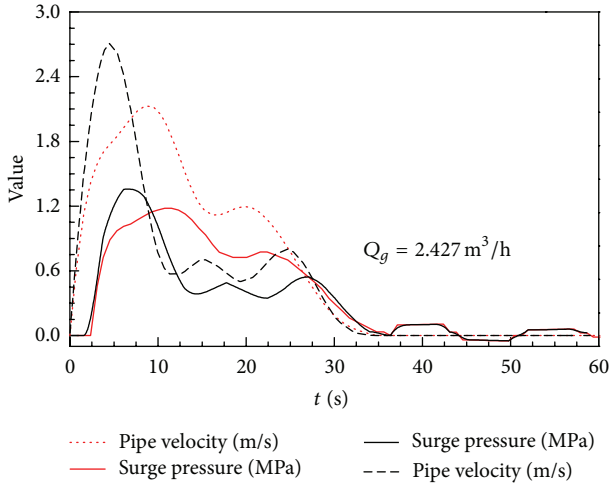

Figure 21: Surge pressure variations at different pipe velocities (gas influx Q_g = 2.427 m^3/h).

mass conservation equations, the momentum conservation equations, characteristic line method, and the gas-drilling mud equations of state (EOS) during MPD operations. Solved by the difference method and fourth-order explicit Runge-Kutta method, the model is used to predict surge pressure for different drill pipe operating speed and gas influx rates in MPD operations. The main conclusions can be summarized as follows.

(1) An accurate mathematical model to predict surge pressure after gas influx is of great importance because of the effects of surge pressure on operational safety and success. The new model provides better prediction of surge pressures in comparison with the existing experiment.

(2) The surge pressure tends to increase with the increase of drill pipe operating speed and decrease of gas influx rate and well diameter. Considering that the gas influx occurs, the surge pressure weakens obviously. With the increases in well depth, the maximum allowable tripping speed gradually become smaller, the surge pressure increases at the bottom of well, and drilling safety window is accordingly narrower. The surge pressure can cause a significant time lag if the gas influx occurs at the bottom of well, and the time lag is mainly determined by the propagation time of pressure wave in the wellbore.

(3) The surge pressure obviously varies at different scenarios (OPOP, CPOP, and OPWP, resp.) during the tripping operations. Surge pressure increased in CPOP scenario than in OPOP scenario. Especially when the maximum surge pressure occurs, a strong increase of surge pressure is observed at OPWP scenario. By running the new surge pressure model, drilling engineers can identify potential surge problems and optimize tripping operations for different scenarios as to avoid complicated accidents to happen in wellbore during drilling operations.

(4) The calculation of surge pressure in gas drilling mud two-phase is more complex than conventional calculation in single drilling mud. Drill pipe operating speed in drilling operations should be strictly controlled, and the surge pressure should be considered in the design. The greatest advantages of new model are the ability to reduce nonproductive time (NPT) in drilling.

Nomenclature

A: Wellbore effective cross-area (m^2)
A_0: The outer drill pipe cross-area (m^2)
A_2: Wellbore cross-area (m^2)
A_3: The inner Drill pipe cross-area (m^2)
A_e: Effective cross-area of jet nozzle (m^2)
c: Wave velocity (m/s)
ds: One discrete length of wellbore (m)

D: Wellbore effective diameter (m)
D_1: The inner diameter of casing (m)
D_2: The outer diameter of casing (m)
D_3: The inner diameter of drill pipe (m)
D_4: The outer diameter of drill pipe (m)
D_{kj}: Differential equation coefficients
E_{kj}: Differential equation coefficients
E_s: Modulus of elasticity of the drill pipe (MPa)
E_f: Modulus of elasticity of formation (MPa)
E_2: Modulus of elasticity of casing (MPa)
f_G: Shear stresses coefficient of gas interface
f: Friction coefficient
f_2: Wellbore friction coefficient
f_3: Drill pipe friction coefficient
f_L: Shear stresses coefficient of drilling mud
F_z: Pressure applied on the two-phase flow (N)
g: Acceleration due to gravity (m^2/s)
g_c: Conversion factor
g_T: Geothermal temperature gradient (K/m)
k_e: Wellbore effective roughness (m)
k_0: Roughness of outer pipe (m)
k_i: Roughness of inner pipe (m)
H: The depth of well (m)
L_1: The length from pipe bottom to hole bottom (m)
L_2: The length from pipe bottom to well head (m)
Lg: Flow pattern
m: Hydraulic radius (m)
m_2: Wellbore hydraulic radius (m)
m_3: Drill pipe hydraulic radius (m)
N: Parameter combining Thompson energy effects
P: Pressure (MPa)
P_0: Initial pressure of wellbore (MPa)
P_2: Pressure within the empty wellbore (MPa)
P_3: Pressure within the drill pipe (MPa)
P_c: Critical pressure (kPa)
P_L: Pressure of drilling mud (MPa)
P_r: Reduced pressure
P_{jt}: Pressure at node (j, t) (MPa)
q_m: Volumetric flow rate of two phase (m^3/s)
q_G: Velocity of the gas (m^3/s)
q_L: Velocity of the drilling mud (m^3/s)
Q_L: Mud flow rate within the wellbore (m^3/h)
Q_1: Drilling mud flow rate within hole (m^3/h)
Q_2: Mud flow rate within the wellbore (m^3/h)
Q_3: Mud flow rate within the drill pipe (m^3/h)
Q_w: Pump flow rate (m^3/s)
Q_{jt}: Flow rate at time t and nod j (m^3/s)
R: Constant of EOS (J/KgK)
s: The length of wellbore along wellbore (m)
t: Time (s)
T: Temperature (K)
T_c: Critical temperature (K)
T_r: Reduced temperature
T_{ei}: Undistributed temperature at a depth (K)
T_{ebh}: Undistributed temperature of wellhead (K)
T_{fbh}: Undistributed temperature at bottom-hole (K)
v: Velocity of drilling mud and gas (m/s)
v_p: Velocity of drill pipe (m/s)
v_m: Gas and drilling mud flow velocity (m/s)
v_G: Gas flow velocity (m/s)
v_s: Slip velocity (m/s)
v_{sg}: Superficial gas velocity (m/s)
v_L: Drilling mud flow velocity (m/s)
W_m: Mass flow velocity (kg/m^3)
z_G: Gas deviation factor
z_0: Initial calculation height of wellbore (m)
z_{bh}: Total well depth from surface (m)
z: Variable of distance from surface (m).

Greek Letters

ρ_G: Gas density (kg/m^3)
τ_f: Frictional pressure gradient (Pa/m)
τ_w: Frictional pressure coefficient
ρ_m: Gas and drilling density (kg/m^3)
ρ_0: Density under atmospheric pressure (kg/m^3)
ρ_L: Drilling mud density (kg/m^3)
σ_s: Surface tension (N/m^2)
ϕ_G: Gas void fraction
ϕ_L: Drilling mud holdup
ρ_r: Reduced density
μ_L: Viscosity of drilling mud (Pa·s)
θ: The ground angle (rad)
μ_f: Poisson's ratio of formation
μ_s: Poisson's ratio of drill pipe
μ_2: Poisson's ratio of casing
ΔA: The change of the across areas (m^2).

Subscripts

CPOP: Closed pipe without pumping
DAPC: Dynamic annular pressure control
EOS: Equations of state
ERV: Relief-coupling valve
MPD: Managed pressure drilling
OPOP: Open pipe without pumping
OPWP: Open pipe with pumping
R-K4: The fourth-order explicit Runge-Kutta
RCD: The rotating control device.

Subscripts of Graph

c: Wave velocity in two-phase flow (m/s)
D: Wellbore effective diameter (m)
H: Depth of wellbore (m)
L: The length from drill pipe and drill pipe (m)
Q_g: Gas influx rate at the bottomhole (m^3/h)
ϕ_G: Void fraction (%).

Conflict of Interests

The authors declare that there is no conflict of interests regarding the publication of this paper.

Acknowledgments

This research work was cofinanced by the National Natural Science Foundation of China (nos. 51074135, 51274170, and QC2012C128). Without their support, this work would not have been possible.

References

[1] Y. Bu, F. Li, Z. Wang, and J. Li, "Preliminary study of Air Injection in Annuli to manage pressure during Cementing," *Procedia Engineering*, vol. 18, pp. 329–334, 2011.

[2] W. Guo, F. Honghai, and L. Gang, "Design and calculation of a MPD model with constant bottom hole pressure," *Petroleum Exploration and Development*, vol. 38, no. 1, pp. 103–108, 2011.

[3] S. Saeed and R. Lovorn, "Automated drilling systems for MPD—the reality," in *Proceedings of the IADC/SPE Drilling Conference and Exhibition*, San Diego, Calif, USA, March 2012.

[4] P. Vieira, F. Torres, R. A. Qamar, and G. E. Marin, "Downhole pressure uncertainties related to deep wells drilling are safely and precisely ascertained using automated MPD technology," in *Proceedings of the Norh Africa Technical Conference and Exhibition*, Cairo, Egypt, February 2012.

[5] J. Saponja, A. Adeleye, and B. Hucik, "Managed-pressure drilling (MPD) field trials demonstrate technology value," in *Proceedings of the IADC/SPE Drilling Conference*, Miami, Fla, USA, February 2006.

[6] G. Liu, "Predicting surge pressures that result from running liners," *World Oil*, vol. 222, no. 4, p. 92, 2001.

[7] K. Zhou, J. Yang, B. Zhong, and L. Tang, "Surge pressure in wellbore," *Oil Drilling and Production Technology*, vol. 12, no. 2, pp. 1–10, 99, 1990.

[8] R. S. Rudi Rubiandini, "New formula of surge pressure for determining safe trip velocities," in *Proceedings of the SPE Asia Pacific Oil and Gas Conference and Exhibition*, pp. 16–18, aus, October 2000.

[9] J. Li, Z. Huang, K. Li, and W. Wu, "The influence of collar on surge pressure caused by the drilling fluid viscous force under pumping condition," *Research Journal of Applied Sciences, Engineering and Technology*, vol. 5, no. 5, pp. 1781–1785, 2040–7459, 2013.

[10] S. Wang, C. Qiang, and K. Bo, "Fluctuating pressure calculation during the progress of trip in managed pressure drilling," *Advanced Materials Research*, vol. 468–471, pp. 1736–1742, 2012.

[11] F. Crespo and R. Ahmed, "Surge-and-swab pressure predictions for yield-power-law drilling fluids," *SPE Drilling & Completion*, vol. 27, no. 4, pp. 574–585, 2012.

[12] H. Wang and X. Liu, "Study on steady surge pressure of casson fluid in concentric wellbore of directional wells," *Drilling Fluid Completion Fluid*, vol. 11, no. 6, pp. 35–40, 44, 79, 1994.

[13] G. A. Chukwu, "Surge and swab pressure computed for couette flow of power-law fluids," *PHD Thesis*, vol. 50, no. 9, p. 143, 1989.

[14] H. Fan, "Development of application software for dynamic surge pressure while tripping," *Petroleum Drilling and Technology*, vol. 23, no. 4, pp. 11–14, 1995.

[15] K. Zhou, J. Yang, B. Zhong, and L. Tang, "Surge pressure in wellbore," *Journal of Petroleum Exploration and Production Technology*, vol. 12, no. 2, pp. 1–10, 1990.

[16] G. A. Chukwu, "Surge and swab pressure computed for couette flow of power-law fluids," *Dissertation Abstracts International B*, vol. 50, no. 9, 1989.

[17] Z. Jiang, "Studies of wellbore surge pressure by a dynamic method," *Journal of Petroleum Exploration and Production Technology*, vol. 13, no. 3, pp. 39–44, 97, 1991.

[18] H. Wang and X. Liu, "Study on steady surge pressure of casson fluid in concentric wellbore of directional wells," *Drilling Fluid Completion Fluid*, vol. 11, no. 6, pp. 35–40, 44, 79, 1994.

[19] D. Johnston, M. Bracken, and J. Thornton, "Assessing pipe condition, useful remaining life and maximum operating and surge pressures: when to change the pipe or control the pressure," *Magazine of the International Water Association*, vol. 14, no. 5, pp. 43–44, 2012.

[20] H. Fan, Y. Chu, and X. Liu, "Prediction for wellbore dynamic surge pressure while tripping a drill pipe," *Journal of China University of Petroleum*, vol. 19, no. 5, pp. 36–41, 1995.

[21] C. K. Burgess, J. E. Miller, and K. D. Vondervort, "Downhole surge pressure reduction system and method of use," World 98/48 143, 1998.

[22] J. P. Allamon, J. E. Miller, and A. M. Macfarlane, "Downhole Surge Reduction Method and Apparatus," 2004.

[23] K. S. Bjørkevoll, R. Rommetveit, B. Aas, H. Gjeraldstveit, and A. Merlo, "Transient gel breaking model for critical wells applications with field data verification," in *Proceedings of the 2003 Offshore Mediterranean Conference*, February 2003.

[24] G. H. Nygaard, E. Johannessen, J. E. Gravdal, and F. Iversen, "Automatic coordinated control of pump rates and choke valve for compensating pressure fluctuations during surge and swab operations," in *Proceedings of the IADC/SPE Managed Pressure Drilling and Underbalanced Operations Conference*, pp. 120–125, March 2007.

[25] J. V. Fedevjcyk, S. L. M. Junqueira, and C. O. R. Negrão, "Surge & swab pressures in wells with cross-section changes," *Boletim Tecnico da Producao de Petroleo*, vol. 4, no. 2, pp. 221–234, 2009.

[26] S. Tian, G. H. Medley, and C. R. Stone, "Understanding yield point: effect onpressure surges critical to managing deep, difficult MPD wells," *Drilling Contractor*, vol. 65, no. 4, p. 46, 48, 50, 53, 2009.

[27] Y. Sun, Q. Li, and J. Zhao, "New method of predicting surge pressure apply to horizontal well based on caisson flow," *Natural Science*, vol. 2, no. 12, pp. 1394–1399, 2150–4091, 2010.

[28] B. T. Lebele-Alawa and F. E. Oparadike, "Analysis of the effects of valve propagated pressure surge on pipe flow," *Engineering*, vol. 3, no. 11, pp. 1098–1101, 2011.

[29] X. Kong, Q. Yuan, and Y. Qiu, "The research of two-phase fluctuation pressure in wellbore tripping operation," *Inner Mongolia Petrochemical Industry*, TE242, 2011.

[30] F. Crespo and R. Ahmed, "A simplified surge and swab pressure model for yield power law fluids," *Journal of Petroleum Science and Engineering*, vol. 101, pp. 12–20, 2013.

[31] F. Huang, M. Takahashi, and L. Guo, "Pressure wave propagation in air-water bubbly and slug flow," *Progress in Nuclear Energy*, vol. 47, no. 1–4, pp. 648–655, 2005.

[32] P. M. Dranchuk and J. H. Abou-Kassem, "Calculation of Z factors natural gases using equitation of state," *Journal of Canadian Petroleum Technology*, vol. 14, no. 3, pp. 34–36, 1975.

[33] A. R. Hasan and C. S. Kabir, "Wellbore heat-transfer modeling and applications," *Journal of Petroleum Science and Engineering*, vol. 86-87, pp. 127–136, 2012.

[34] J. Orkiszewski, "Predicting two-phase pressure drops in vertical pipe," *Journal of Petroleum Technology*, vol. 6, no. 6, pp. 829–838, 1967.

[35] M. J. Sanchez, *Comparison of Correlations for Predicting Pressure Losses in Vertical Multiphase Annular Flow*, University of Tulsa, Tulsa, Okla, USA, 1972.

[36] H. Li, Y. Meng, G. Li et al., "Propagation of measurement-while-drilling mud pulse during high temperature deep well drilling operations," *Mathematical Problems in Engineering*, vol. 2013, Article ID 243670, 12 pages, 2013.

[37] Y. Lin, X. Kong, Y. Qiu, and Q. Yuan, "Calculation analysis of pressure wave velocity in gas and drilling mud two-phase fluid in annulus during drilling operations," *Mathematical Problems in Engineering*, vol. 2013, Article ID 318912, 17 pages, 2013.

[38] H. Zhu, Y. Lin, D. Zeng, D. Zhang, and F. Wang, "Calculation analysis of sustained casing pressure in gas wells," *Petroleum Science*, vol. 9, no. 1, pp. 66–74, 2012.

[39] H. Junfang, "Balanced drilling and well control," *Petroleum Industry Press*, vol. 1, article 33, 1992.

[40] W. A. Bacon, *Consideration of compressibility effects for applied-back- pressure dynamic well control response to a gas kick in managed pressure drilling operations [M.S. thesis]*, University of Texas, Arlington, Va, USA, 2011.